Ecological Indicators 89 (2018) 808–817

Contents lists available at ScienceDirect

Ecological Indicators

journal homepage: www.elsevier.com/locate/ecolind

Original Articles

When and where to reduce nutrient for controlling harmful algal blooms in large eutrophic lake Chaohu, China?

Jiacong Huang[a,b], Yinjun Zhang[c], Qi Huang[d], Junfeng Gao[a,*]

[a] Key Laboratory of Watershed Geographic Sciences, Nanjing Institute of Geography and Limnology, Chinese Academy of Sciences, 73 East Beijing Road, Nanjing 210008, China
[b] Ecological Modelling Laboratory, Department of Physical & Environmental Sciences, University of Toronto, Toronto, ON M1C 1A4, Canada
[c] China National Environmental Monitoring Centre, 8(B) Dayangfang Beiyuan Road, Chaoyang District, Beijing 100012, China
[d] Key Laboratory of Poyang Lake Wetland and Watershed Research, Ministry of Education, Jiangxi Normal University, Nanchang 330022, China

ARTICLE INFO

Keywords:
Harmful algal blooms (HABs)
Phosphorus loading
Environmental fluid dynamics code (EFDC)
Lake Chaohu

ABSTRACT

Nutrient reduction was an important but costly strategy to control harmful algal blooms (HABs) in eutrophic lakes. It is still unclear that when and where to reduce nutrients for controlling HABs in a large eutrophic lake. This study proposed a nutrient loading contribution index (NLCI) to evaluate the contribution of nutrient loading on HABs in a large eutrophic lake (Lake Chaohu, China). The index was calculated using a hydrological, hydrodynamic and water quality model. A multi-site and multi-variable calibration revealed that the coupled model captured the spatio-temporal pattern of chlorophyll *a* in the lake representing HABs. The evaluation results revealed that effective HABs controlling in the lake depended on reducing P loading. Both internal and external P loading contributed significantly to HABs in the lake. Nanfei and Hangbu Rivers were the hot spots for external P reduction. Aug., May and Jul. were the hot moments for external P reduction. The new index (NLCI) can be potentially used in other large eutrophic lakes to make a better strategy for nutrient reduction in water management practice.

Model availability

Model name: Xinanjiang Model
Model download: http://www.escience.cn/people/elake/index.html
Programming language: Python
Model name: Environmental Fluid Dynamics Code (EFDC)
Model download: http://sourceforge.net/projects/snl-efdc/
Programming language: FORTRAN

1. Introduction

Harmful algal blooms (HABs) caused by excessive nutrient loading in freshwater systems have been a global problem for decades. Examples of severe HABs included Lakes Taihu and Chaohu in China (Kong et al., 2017; Qin et al., 2010), Lake Erie in North America (Michalak et al., 2013; Watson et al., 2016), Lake Winnipeg in Canada (Schindler et al., 2012; Ulrich et al., 2016). These HABs caused the harmful impacts of oxygen depletion, fish kills, liver damage by toxins, biodiversity loss and water quality degradation (Catherine et al., 2013; Clark et al., 2017; Paerl and Huisman, 2008). Reducing nitrogen (N) and phosphorus (P) loadings can limit excessive phytoplankton growth (Brookes and Carey, 2011), and had achieved great success for controlling HABs in many freshwater lakes, such as Lake Erie in North America (Smith et al., 2015). However, decision-making on nutrient reduction was challenging for a large lake due to the following unaddressed questions.

(1) Whether one or both nutrients should be reduced for controlling HABs? Inspired by Liebig's minimum law, worldwide limnologists have been trying to identify the most limiting nutrient for phytoplankton growth in eutrophic lakes. P was found to be the growth-limiting nutrient, and P controlling was thus strongly recommended (Hecky and Kilham, 1988; Imboden and Gachter, 1978; Thomas, 1972; Vollenweider, 1976). This conclusion led to widespread of P loading

Abbreviations: NLCI, nutrient loading contribution index; HABs, harmful algal blooms; EFDC, environmental fluid dynamics code; Q, flow discharge (m^3/s); WL, water level (m); TP, total phosphorus (mg P/L); TN, total nitrogen (mg N/L); NH_4^+, ammonia nitrogen (mg N/L); CHL, Chlorophyll *a* (μg/L); DO, dissolved oxygen (mg/L); WT, water temperature (°C)

* Corresponding author.
E-mail addresses: jchuang@niglas.ac.cn (J. Huang), gaojunf@niglas.ac.cn (J. Gao).

https://doi.org/10.1016/j.ecolind.2018.01.056
Received 14 August 2017; Received in revised form 23 January 2018; Accepted 24 January 2018

reductions in North American and European lakes and consequent improvements in water quality (National Research Council, 1992). However, a dual (N and P) nutrient reduction was proposed in some lakes that were dominated by non-N_2-fixing cyanobacteria, and had a rapid P recycle between water and sediment (Conley et al., 2009). Although hot debates among N or P reduction to control HABs are continuing (Conley et al., 2009; Schindler, 1974), there is a consensus that an appropriate strategy for nutrient (N or P) controlling can be determined by investigating N:P ratios using Redfield ratio (Abell et al., 2010; Schindler et al., 2008), that was originally proposed by Alfred C. Redfield in 1934 (Arrigo, 2014).

(2) When and where to reduce nutrients for controlling HABs? Nutrient reduction is one of the most effective strategies to control HABs for a eutrophic lake (Schindler et al., 2016). However, either internal or external nutrient loading reduction is time-consuming and costly. Therefore, learning the nutrient contribution to HABs in the lake can help water managers to make a priority list on nutrient reduction. Successful cases to investigate the response of HABs/phytoplankton to nutrient conditions were implemented in many aquatic ecosystems, such as Lake Taihu (Huang et al., 2016), Lake Dianchi (Wu et al., 2017) and the Bay of Quinte, Lake Ontario (Shimoda et al., 2016). However, for large lakes, a specific nutrient reduction strategy (e.g., P reduction from one inflow) may alleviate HABs in different areas to different extents. Therefore, it is helpful for water managers to know when and where to reduce nutrients for controlling HABs in the most concerned area (e.g., drinking water intake). To our knowledge, this question was scarcely investigated for a large shallow lake due to its multiple nutrient sources and complex mass transport processes.

The hypothesis of this study was that nutrient reduction in different inflows and during different periods would result in different spatio-temporal patterns of HABs in a large shallow lake. To test above hypothesis, a large shallow eutrophic lake (Lake Chaohu) in China was used as an example. A new nutrient loading contribution index (NLCI) was proposed to evaluate nutrient loading contribution to spatio-temporal pattern of HABs. NLCI had the advantage of describing HABs and nutrient transport in the large lake using a hydrological, hydrodynamic and water quality model. Based on the evaluation results using NLCI, the contribution of nutrient sources (inflows and sediment fluxes) for spatio-temporal pattern of HABs in the lake was accounted for.

2. Materials and methods

2.1. Study area and data

Lake Chaohu (surface area, 768 km^2; mean depth, 2.7 m), the fifth largest freshwater lake in China, is located in central Lake Chaohu watershed (13,555 km^2) (Fig. 1). The main connecting rivers of Lake Chaohu include six inflows (Hangbu, Baishitian, Zhao, Zhegao, Nanfei and Pai Rivers) and one outflow (Yuxi River) connecting with Yangtze River. A sluice at H3 was used to control water level of Lake Chaohu since Dec. 1962, and resulted in a long water retention time of 207 d, and a large water level fluctuation from 8.11 m to 10.04 m above sea level (Wusong datum) during 2011–2014. Lake Chaohu was well-known for its scenic beauty and rich aquatic products before the 1960s. However, due to rapid population growth and economic development during past few decades, Lake Chaohu showed a decreasing trend of wetland area, macrophyte coverage, and an increasing trend of algal biomass (Xu et al., 1999). HABs occurred from May to November since 1980s. During the past decade, a series of measures (e.g., improving wastewater treatment) have been taken by government to control eutrophication in Lake Chaohu. However, HABs coverage, frequency, and duration showed an increasing trend during 2000–2013 (Zhang et al., 2015). The phytoplankton was dominant by cyanobacteria (99.5% of total phytoplankton biomass) (Jiang et al., 2014). Nutrients (phosphorus and nitrogen) and HABs in western Lake Chaohu were significantly higher than those in eastern Lake Chaohu (Zhang et al., 2016). Nonpoint source pollution from agricultural farmlands was found to be the primary nutrient sources for the lake (Zhou and Gao, 2011).

A measured dataset was collected during 2010–2014 for modeling HABs in Lake Chaohu (Table 1). This dataset included land use, meteorological, hydrological and water quality data. The land use data were derived from satellite images (the moderate-resolution imaging spectroradiometer, MODIS) in 2010. The daily meteorological data were collected from six national weather stations and a hydrological station. The daily hydrological data including flow discharge (Q, m^3/s) and water level (WL, m). Q data were collected from three hydrological stations of H1, H2 and H3. WL data were collected from the hydrological station of H3. Water quality data included the variables of total

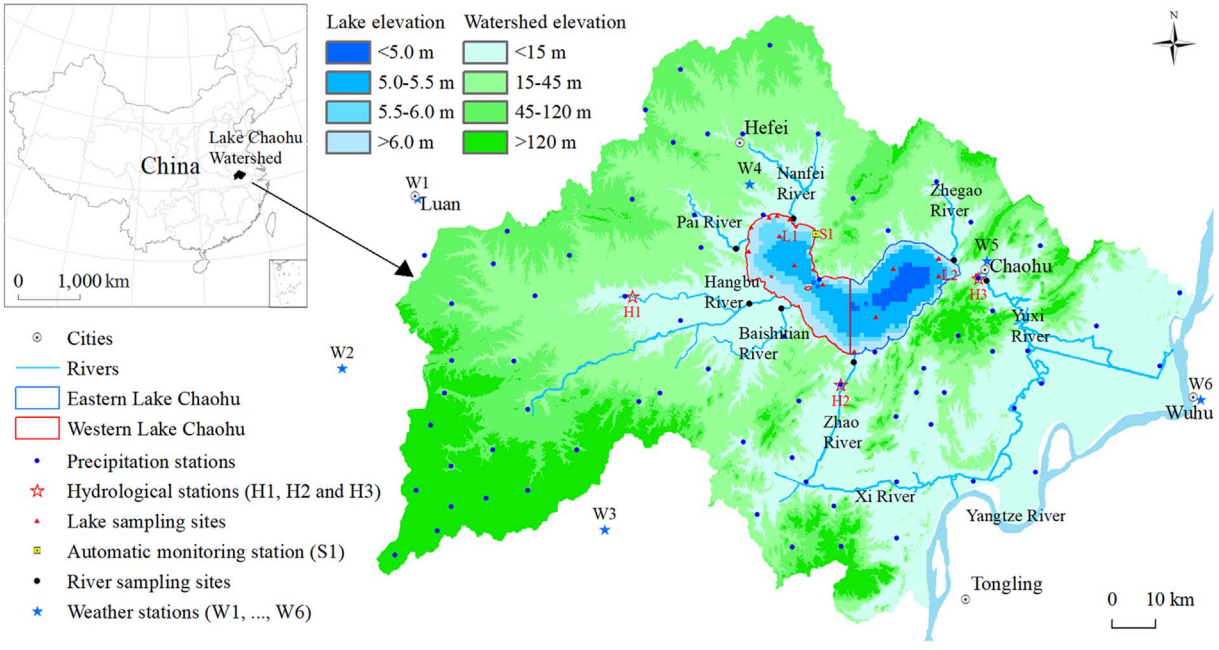

Fig. 1. Locations of Lake Chaohu watershed, elevation above sea level (Wusong datum), river network, water sampling sites, weather and hydrological stations.

Table 1
Data collected for modeling harmful algal blooms in Lake Chaohu.

Type	Indicator	Time period	Temporal resolution	Source	Use
Land use	Land use type	2010		Satellite image	Inputs
Meteorology	Pr	2010–2014	Daily	72 precipitation stations	Inputs
	T_{Max}, T_{Min}, T_{Ave}, Wet, WS and H_{Sun}	2010–2014	Daily	Weather stations (W1, …, W6)	Inputs
	EV	2010–2014	Daily	Hydrological station (H1)	Inputs
Hydrology	Q	2010–2014	Daily	Hydrological stations (H1, H2 and H3)	Calibration
	WL	2010–2014	Daily	Hydrological station (H3)	Calibration
Water quality	TP, TN, NH_4^+ and CHL	2010–2014	Monthly	7 river water sampling sites	Inputs
	TP, TN, NH_4^+ and CHL	2010–2014	Monthly	14 lake water sampling sites	Calibration
	DO and WT	2010–2014	6 h	Automatic monitoring station (S1)	Calibration

Note: Locations for data sources can be found in Fig. 1. WL: water level (m); Q: flow discharge (m^3/s); Pr: daily precipitation (mm); T_{Max}, T_{Min} and T_{Ave}: daily maximum, minimum and average of air temperature (°C); Wet: daily average humidity (%); WS: daily average wind speed (m/s); H_{Sun}: daily sunshine hours (h); TP: total phosphorus concentration (mg P/L); TN: total nitrogen concentration (mg N/L); NH_4^+: ammonia nitrogen concentration (mg N/L). CHL: chlorophyll *a* concentration (μg/L); DO: dissolved oxygen (mg/L); WT: water temperature (°C).

phosphorus (TP, mg P/L), total nitrogen (TN, mg N/L), ammonia nitrogen (NH_4^+, mg N/L), chlorophyll *a* (CHL, μg/L), dissolved oxygen (DO, mg/L) and water temperature (WT, °C). TP, TN, NH_4^+ and CHL data were obtained from monthly water sampling in the lake, the six inflows and one outflow. DO and WT was measured every 6 h using automatic and high frequency monitoring sensors at the automatic monitoring station of S1.

2.2. Model descriptions

HABs in Lake Chaohu were simulated using a coupled hydrological, hydrodynamic and water quality model (Fig. 2). The hydrological model (Xinanjiang model) aimed to simulate daily inflow discharge for the hydrodynamic and water quality model (Environmental Fluid Dynamics Code, EFDC). Further details on these two models were presented in Sections 2.2.1 and 2.2.2, respectively. The hydrodynamic and water quality model aimed to simulate the spatio-temporal pattern of HABs. HABs were caused by explosive growth of phytoplankton (Brookes and Carey, 2011), and was thus represented using CHL in this study. The simulation period was 2010–2014 with the warm-up period of 2010 and the calibration period of 2011–2014.

2.2.1. Raster-based hydrological model

Xinanjiang model originally developed by Zhao (1992) was used to simulate daily discharge of five inflows for Lake Chaohu including Hangbu, Baishitian, Zhegao, Nanfei and Pai Rivers (Fig. 1). The raster-based hydrological model included four modules, i.e., evapotranspiration module, runoff generation module, runoff separation module and runoff routing module. Water evapotranspiration was calculated based on the Penman–Monteith method proposed by Allen et al. (1998). A parabolic curve of tension water capacity was used to describe the watershed heterogeneity in runoff generation module. Runoff separation module divided the total runoff into three components, including surface runoff, interflow and groundwater runoffs. Runoff routing

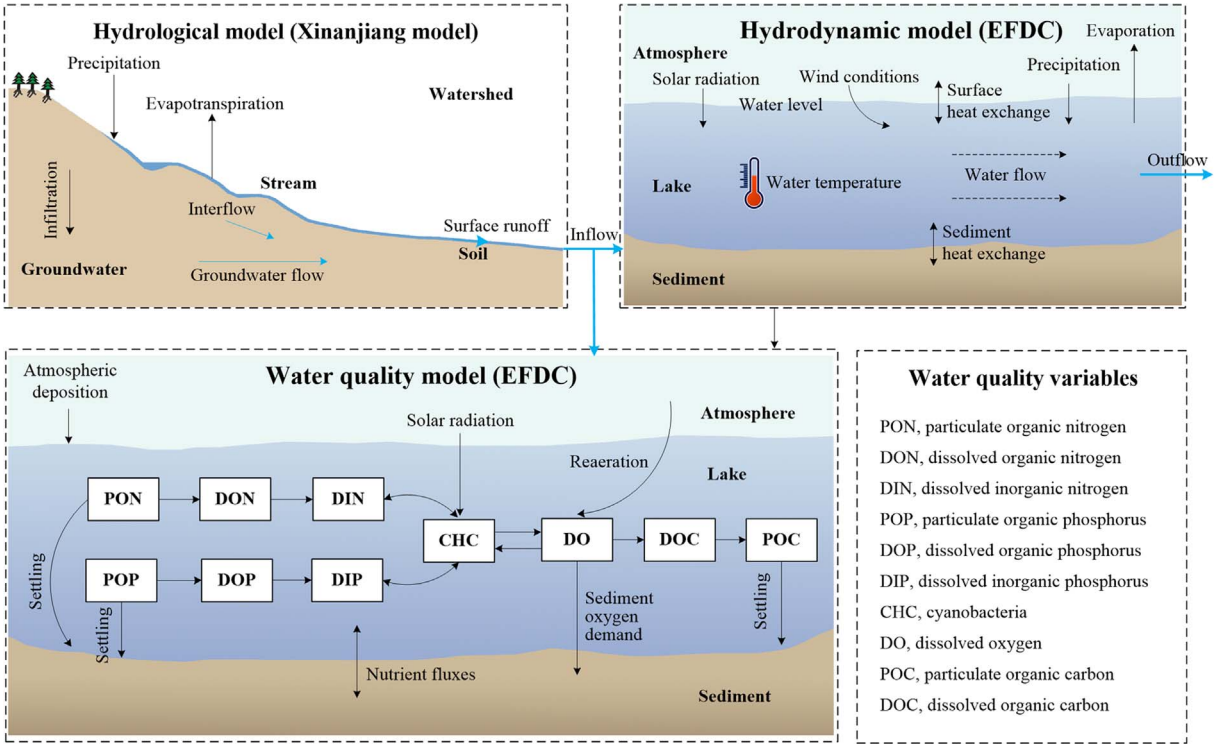

Fig. 2. Conceptual diagram for modeling harmful algal blooms (HABs) in Lake Chaohu. Xinanjiang model is a raster-based hydrological model (See Section 2.2.1). EFDC (Environmental Fluid Dynamics Code) is a three-dimensional hydrodynamic and water quality model (See Section 2.2.2).

module described the overland and channel flow by the one-dimensional kinematic wave function with Manning's equation. The hydrological model used a daily time step and a spatial resolution of 500 m, with a total of 54,220 cells for the watershed. Further details about the Xinanjiang model can be found in many previous studies (Zhao et al., 2011; Zhao, 1992).

2.2.2. Three-dimensional hydrodynamic and water quality model

The hydrodynamic and water quality model (EFDC), originally developed by Hamrick (1996), was used to simulate hydrodynamic (water temperature and velocity) and water quality (phosphorus, nitrogen, carbon and phytoplankton) dynamics in Lake Chaohu. EFDC solves three-dimensional, vertically-hydrostatic, free-surface and turbulent-averaged equations of motion for a variable-density fluid, and has been widely used in various aquatic ecosystems (Arifin et al., 2016; Du and Shen, 2016; Huang et al., 2017; Tang et al., 2017). The governing mass-balance equation for each of the water quality state variables can be expressed as (Tetra Tech, 2007):

$$\frac{\partial(m_x m_y HC)}{\partial t} + \frac{\partial}{\partial x}(m_y HuC) + \frac{\partial}{\partial y}(m_x HvC) + \frac{\partial}{\partial z}(m_x m_y wC) = \frac{\partial}{\partial x}\left(\frac{m_y HA_x}{m_x}\frac{\partial C}{\partial x}\right) + \frac{\partial}{\partial y}\left(\frac{m_x HA_y}{m_y}\frac{\partial C}{\partial y}\right) + \frac{\partial}{\partial z}\left(m_x m_y \frac{A_z}{H}\frac{\partial C}{\partial z}\right) + m_x m_y HS_c \quad (1)$$

where C is concentration of a water quality state variable. u, v and w are velocity components in the curvilinear, sigma, x-, y- and z-directions, respectively. A_x, A_y and A_z are turbulent diffusivities in the x-, y-, and z-directions, respectively. S_c is internal and external sources and sinks per unit volume. H is water column depth. m_x and m_y are horizontal curvilinear coordinate scale factors. In Eq. (1), the first term on the left-hand side represents the spatial and temporal dynamics of each state variable. The last three terms on the left-hand side account for the advective transport. The first three terms on the right-hand side account for the diffusive transport. The last term describes the kinetic processes and external loads for each state variable.

The model considered phytoplankton kinetics, sediment nutrient fluxes, atmospheric nutrient deposition, phytoplankton and nutrient transport. The kinetic equation for phytoplankton can be expressed as (Tetra Tech, 2007):

$$\frac{\partial B_x}{\partial t} = (P_x - BM_x - PR_x)B_x + \frac{\partial}{\partial Z}(WS_x \times B_x) + \frac{WB_x}{V} \quad (2)$$

where B_x is algal biomass of phytoplankton group x (g C m^{-3}). t is time (d). P_x is production rate of phytoplankton group x (d^{-1}). BM_x is basal metabolism rate of phytoplankton group x (d^{-1}). PR_x is predation rate of phytoplankton group x (d^{-1}). Z is water depth (m). WS_x is positive settling velocity of phytoplankton group x (m d^{-1}). WB_x is external loads of phytoplankton group x (g C d^{-1}). V is cell volume (m^3). Two phytoplankton groups (*Microcystis* and *Anabaena*) were considered in EFDC due to their domination in Lake Chaohu (Zhang et al., 2016).

Sediment nutrient fluxes across the sediment–water interface were simulated using a sediment flux module that was internally coupled with other modules in EFDC (Park et al., 2005). The module incorporates three processes including depositional flux of particulate organic matter, their diagenesis and the resulting sediment flux. The module is driven by net settling of particulate organic carbon and nutrients from the overlying water calculated by the eutrophication model for water column. The module simulates the diagenesis of deposited particulate organic matter, producing inorganic nutrients and oxygen demand as sulfide or methane. The end products of diagenesis exert sediment fluxes of nutrients and sediment oxygen demand depend on the ambient conditions.

EFDC used a time step of 200 s and a spatial resolution of 1 km, with a total of 768 cells in the lake. Compared with the hydrological model (Xinanjiang model), its time step is shorter to increase model stability, while its spatial resolution is larger to reduce computation time. In order to capture the vertical changes of water temperature and velocity, two layers were employed in the vertical direction using a sigma coordinate. Boundary conditions for the hydrodynamic and water quality model included precipitation, wind conditions, flow discharge, inflow water quality and internal nutrient loading. Daily precipitation and wind conditions were obtained from the weather station near the lake (W5 in Fig. 1). Daily discharge data of five inflows were simulated using the hydrological model (Section 2.2.1). Discharge of Zhao and Yuxi Rivers were manually controlled, and was thus obtained from daily measured data at the hydrological stations (H1 and H2 in Fig. 1). Water quality data of six inflows were obtained from monthly measured data at 6 river sampling sites (Fig. 1).

2.2.3. Multi-site and multi-variable calibration

This study implemented a multi-site (five stations: H1, H3, S1, L1 and L2) and multi-variable (eight variables: Q, WL, WT, DO, CHL, TN, NH_4^+ and TP) calibration for the coupled hydrological, hydrodynamic and water quality model using the intensive dataset presented in Section 2.1. More attention was paid to the sensitive parameters identified based on sensitivity analysis (see the Supplementary material). Parameters in three sub-models (the hydrological model, hydrodynamic model and water quality model) were subsequently calibrated based on separate datasets during 2011–2014. The hydrological model was calibrated and validated based on the daily discharge measured at H3 (Fig. 1). The hydrodynamic model was calibrated and validated based on six-hourly WT data measured at S1 (Fig. 1) and daily water level data measured at H2 (Fig. 1). The water quality model was calibrated and validated based on six-hourly DO data measured at S1 (Fig. 1) and monthly TN, NH_4^+, TP and CHL data measured at L1 and L2 (Fig. 1). Model fit was evaluated using the measures of coefficient of determination (R^2) and Nash–Sutcliffe efficiency (NS). R^2 has a value range from 0 (low model fit) to 1 (perfect model fit), while NS has a value range between 1.0 (perfect model fit) and $-\infty$ (low model fit). Further description on R^2 and NS can be found in Krause et al. (2005). The calibrated parameters used in the coupled model can be found in the Supplementary material.

2.3. Evaluating nutrient loading contribution to HABs

Based on nutrient-reduction simulations of the calibrated model, a nutrient loading contribution index (NLCI) was proposed to quantify the impacts of nutrient reduction on HABs. Based on NLCI distribution, nutrient loading contribution maps were derived to show the hot spots and hot moments for nutrient loading for HABs in the lake. Further details on nutrient-reduction simulations, NLCI calculation, mapping nutrient loading contribution were given in the following sections.

2.3.1. Nutrient-reduction simulations

23 simulations were carried out to evaluate the impacts of TP reduction on HABs pattern in Lake Chaohu during 2011–2014 (Table 2). The base simulation (SBase) was carried out to simulate HABs dynamics under present nutrient loading conditions, i.e., without reduction on internal or external nutrient loading. Its simulation results were compared with those from other simulations to evaluate the impacts of TP loading on HABs. Three simulations (SR_0.1, SR_0.2 and SR_0.5) with different reduction of inflow TP loading were carried out to evaluate the impacts of external TP loading on HABs. A simulation (NSR) was carried out to evaluate the impacts of internal TP loading on HABs. Six simulations (SR_i, i = 1, …, 6) were carried out to investigate how TP reduction from different inflows affected HABs. 12 simulations (SR_m, i = 1, …, 12) were carried out to investigate how TP reduction in different months affected HABs. TN-reduction simulations were not carried out in this study because HABs in Lake Chaohu was limited by P rather than N (Section 3.2).

Table 2
Simulations to evaluate the impacts of nutrient reduction on HABs in Lake Chaohu during 2011–2014.

Simulation	Internal nutrient loading	External nutrient loading
SBase	No reduction	No reduction
SR_0.1, SR_0.2 and SR_0.5	No reduction	Reducing six inflows' TP loading by 10%, 20% and 50%, respectively
NSR	Reducing internal TP loading by 50%	No reduction
SR_i (i = 1, …, 6)	No reduction	Reducing TP loading by 50% from all inflows except the ith river[a]
ST_m (m = 1, …, 12)	No reduction	Reducing six inflows' TP loading by 50% all through the year except the mth month[b]

[a] Rivers 1–6 represent six inflows of Hangbu, Baishitian, Zhao, Zhegao, Nanfei and Pai Rivers (Fig. 1).
[b] Months 1–12 represent 12 months (from Jan. to Dec.) in a year.

2.3.2. Nutrient loading contribution index

Based on the 23 nutrient-reduction simulations (Table 2), a nutrient loading contribution index (NLCI) was proposed to quantify the impacts of nutrient reduction from different inflows and seasons on HABs in the lake. NLCI for six inflows and 12 months were defined using the following equations.

$$NLCI_{Ii}^{k} = \frac{CHL_{SR,i}^{k} - CHL_{SR0.5}^{k}}{CHL_{SBase}^{k} - CHL_{SR0.5}^{k}} \quad (3)$$

$$NLCI_{Mm}^{k} = \frac{CHL_{SR,m}^{k} - CHL_{SR0.5}^{k}}{CHL_{SBase}^{k} - CHL_{SR0.5}^{k}} \quad (4)$$

$NLCI_{Ii}^{k}$ was the NLCI values for cell k (k = 1, …, 768) and inflow i (i = 1, …, 6). $CHL_{SR,i}^{k}$ was the simulated annual CHL for cell k with 50% reduction on TP loading from all inflows except inflow i. $CHL_{SR0.5}^{k}$ was the simulated annual CHL for cell k with 50% reduction on TP loading from all inflows. CHL_{SBase}^{k} was the simulated annual CHL for cell k without TP loading reduction. $NLCI_{Mm}^{k}$ was the NLCI values for cell k and month m (m = 1, …, 12). $CHL_{SR,m}^{k}$ was the simulated annual CHL for cell k with 50% reduction on TP loading all through the year except the month m. The values of $CHL_{SR,i}^{k}$, $CHL_{SR,m}^{k}$, CHL_{SBase}^{k} and $CHL_{SR0.5}^{k}$ were obtained from the simulations of SR_i, SR_m, SBase and SR_0.5 (Table 2), respectively.

NLCI was an explicit quantitative definition of the relative contribution of nutrient reduction on HABs. The distinct advantage of the index was its consideration of HABs and nutrient transport process, implying its well suit to use in a large lake. It had a value range from 0 to 1. A $NLCI_{Ii}^{k}$ value of 0 implied that the simulation CHL in cell k from SR_i and SR_0.5 were identical. That is to say, nutrient reduction from inflow i had no impact on CHL in cell k. A higher $NLCI_{Ii}^{k}$ value meant that TP loading from inflow i had a larger impact on CHL in cell k. A higher $NLCI_{Mm}^{k}$ value meant that TP loading in month m has a larger impact on CHL in cell k. The simulation of SR_0.5, rather than SR_0.1 and SR_0.2, was used in the Eqs. (3) and (4) to guarantee a significant difference between its CHL-simulation ($CHL_{SR0.5}^{k}$) and the CHL-simulation (CHL_{SBase}^{k}) from SBase.

Based on the calculated $NLCI_{Ii}^{k}$ and $NLCI_{Mm}^{k}$ (Eqs. (3) and (4)), we used the concept of "hot spots and hot moments" to evaluate the nutrient loading contribution to HABs. Hot spots and hot moments were widely used to describe the spots and short periods with high biogeochemical reaction rates (Andrews et al., 2011). Similarly, hot spots of nutrient loading were defined in this study as spots (inflows and sediment) where nutrient loading had the largest contribution to HABs compared with other spots. Hot moments of nutrient loading were defined as time periods when nutrient loading had the largest contribution to HABs compared with other time periods.

2.3.3. Mapping nutrient loading contribution

Based on Eqs. (3) and (4) (Section 2.3.2), six maps were derived to represent the NLCI values for six inflows. Another 12 maps were derived to represent the NLCI values for 12 months. These maps revealed the nutrient loading contribution of six inflows in different months. However, in water management practice, further questions may be raised such as, which inflow is the most important for reducing nutrient loading to control HABs in a specific area? To answer such question, a map was generated by comparing the relative importance of nutrient reduction from these six inflows using the following equation.

$$M_{I}^{k} = i | NLCI_{Ii}^{k} = \max(NLCI_{I1}^{k},...,NLCI_{I6}^{k}) \quad (5)$$

where M_{I}^{k} represented the most important inflow for nutrient reduction to control HABs in cell k. Similar to the map generating using Eq. (5), another map was generated by comparing the relative importance of nutrient reduction during 12 months using the following equation.

$$M_{M}^{k} = m | NLCI_{Mm}^{k} = \max(NLCI_{M1}^{k},...,NLCI_{M12}^{k}) \quad (6)$$

M_{M}^{k} represented the most important month for nutrient reduction to control HABs in cell k.

3. Results

3.1. Model performance

The multi-site and multi-variable calibration (Section 2.2.3) showed that the coupled hydrological, hydrodynamic and water quality model had an acceptable performance on simulating the seasonal changes of hydrodynamic and water quality conditions (Fig. 3). Both discharge and water level were well simulated with a *NS* value of 0.80 and 0.74. Some discharge peaks during 2014 were not well simulated. Water level during the summer of 2013 was under estimated. Water temperature was perfectly simulated with a *NS* and R^2 value of 0.97 and 0.96. The coupled model captured the seasonal trend of DO, i.e., increasing trend from summer to winter and decreasing trend from winter to summer. However, the large short-term fluctuation of DO was not well simulated, especially during summer period. Spatial heterogeneity and seasonal change of CHL was captured. Both the measured and simulation results showed that CHL in eastern lake was much lower than that in western lake. Some peak values in western lake were not well simulated. Seasonal changes of NH_4^+, TN and TP in the western lake was better simulated than those in the eastern lake. NH_4^+, TN and TP in the western lake had larger value and seasonal fluctuation than those in the eastern lake. The model fit values for CHL, NH_4^+, TN and TP were low mainly due to failure of the model in capturing peak values (Fig. 3).

3.2. Nutrient limitation for HABs

Considering HABs in the western lake (lake sampling site L1) were particularly severe (Fig. 3), its nutrient limitation was investigated. To investigate phytoplankton nutrient limitation, N:P ratio was widely used with a Redfield ratio (7.2:1 weight ratio) to evaluate whether phytoplankton growth was limited by N or P (Schindler et al., 2016; Schindler et al., 2008). A N:P ratio higher than Redfield ratio (weight ratio) implied P limitation for phytoplankton growth. The comparison between simulation and measured N:P ratios in western lake showed a slight over-estimation of N:P ratio. However, it is clear that both simulation and measured N:P ratios were far above Redfield ratio (Fig. 4), implying phytoplankton growth was limited by P rather than

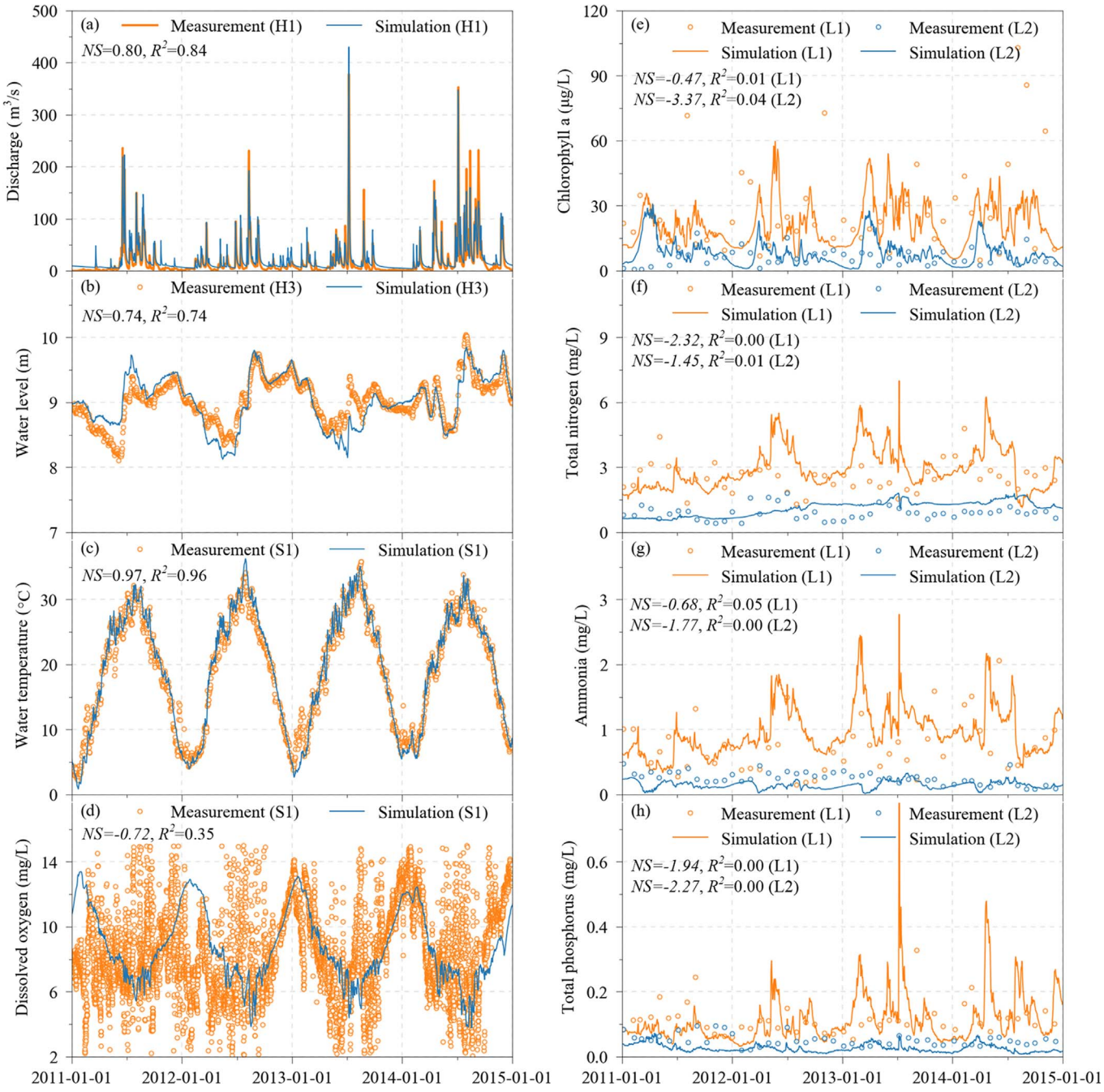

Fig. 3. Measured data and simulation results for the period from Jan.1, 2011 to Dec.31, 2014. (a) Discharge (m^3/s) at H1 (for the geographic location see Fig. 1); (b) Water level (m) at H3; (c) Water temperature (°C) at S1; (d) Dissolved oxygen (mg/L) at S1; (e-h) Chlorophyll *a* (μg/L), total nitrogen (mg/L), ammonia nitrogen (mg/L) and total phosphorus (mg/L) at the lake sampling stations of L1 and L2. R^2, coefficient of determination; *NS*, Nash-Sutcliffe efficiency.

N. During 2011–2014, the average N:P ratio from measured data was 24.4, while the average N:P ratio from simulation results was 32.4 with a large seasonal variation.

3.3. HABs' response to nutrient reduction

3.3.1. Reducing external and internal nutrient loading

The simulation comparison among SBase, SR_0.1, SR_0.2, SR_0.5 and NSR (Table 2) showed that HABs in Lake Chaohu responded differently to external and internal nutrient loading reduction. With internal nutrient loading, inflow nutrient reduction by 50% reduced CHL peak in the eastern lake significantly (Fig. 5(c)), while inflow TP reduction by 10–20% only slightly changed the CHL peak (Fig. 5(a and b)). Inflow TP reduction by 10–50% had slight change of CHL in the eastern lake (Fig. 5(a–c)). With internal TP loading reduced by 50%, the summer CHL peaks in both western and eastern lake were considerably reduced, implying considerable contribution of internal nutrient loading to HABs (Fig. 5(d)).

3.3.2. Reducing nutrient loading from different inflows and months

The NLCI map for six inflows and 12 months (Figs. 6–8) showed that HABs in Lake Chaohu responded differently to nutrient reduction spots and seasons. The NLCI values for six inflows were generally high in their river mouth areas, implying that HABs were significantly affected by inflows. However, the impact of nutrient loading from different inflows on HABs varied significantly. The NLCI values of Hangbu River

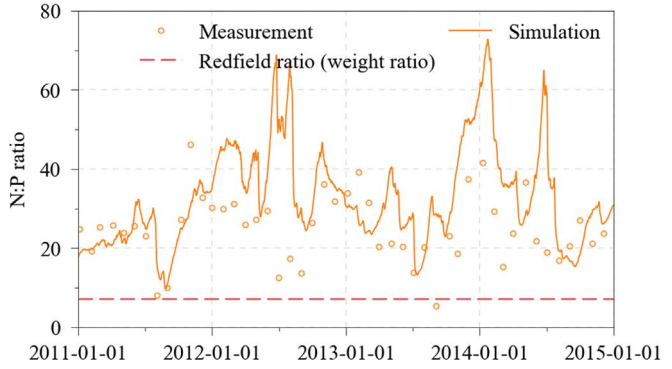

Fig. 4. Monthly N:P ratio with measured data and simulation results at the sampling station L1 for the period from Jan. 1, 2011 to Dec. 31, 2014.

were high in a large area of the lake (Fig. 6(a)). In the western lake, the NLCI values of Nanfei River were much higher than that of other inflows (Fig. 6(e)). HABs in 162 km^2 of the western lake were significantly affected by Nanfei River with its NLCI values higher than 0.4. Other four inflows had low NLCI values except some relatively high values in their river mouth areas.

NLCI values for 12 months varied significantly (Fig. 7). NLCI values for Apr.-Sep. were high implying that HABs in the lake were very sensitive to nutrient reduction in this period. NLCI values for Jan.–Mar. and Oct.–Dec. were generally lower than other months, implying that nutrient reduction during Jan.-Mar. and Oct.–Dec. has less potential to reduce lake HABs compared with nutrient reduction during Apr.–Sep.

Nutrient loading varied significantly among six inflows (see the Supplementary material). Nanfei River had a large nutrient loading (N, 5207.5 t/yr; P, 418.0 t/yr), and had the largest impact for HABs in the western lake (Fig. 8(a)). Nutrient loading from Hangbu River (N, 2738.8 t/yr; P, 228.9 t/yr) had the strongest impact on HABs in eastern lake compared with other inflows (Fig. 8(b)). Other four inflows had relatively low nutrient loading (N, < 1100 t/yr; P, < 80 t/yr), and affected HABs in a small area of their river mouse areas. Nutrient loading had a large fluctuation through time with a large value (N, 1739.8 t/yr; P, 140.5 t/yr) in Jul., and the minimum value (N, 363.8 t/yr; P, 18.6 t/yr) in Jan. (see the Supplementary material). Nutrient reduction in Aug. had the highest potential to reduce HABs in the lake. Nutrient reduction in May and Jul. can potentially reduce HABs in the western lake.

4. Discussion

4.1. Is the coupled model adequate to simulate HABs?

The coupled model was adequate to simulate HABs due to its adequate mechanism to simulate HABs, and acceptable model performance.

(1) Adequate mechanisms to simulate HABs. In the large shallow eutrophic Lake Chaohu, spatio-temporal pattern of HABs can be strongly affected by horizontal phytoplankton transport (Huang et al., 2012), inflow/outflow conditions (Huang et al., 2015), sediment nutrient fluxes (Zhu et al., 2014). The coupled model included adequate mechanism to describe above critical processes for HABs dynamics in Lake Chaohu. The three-dimensional hydrodynamic model was able to describe the horizontal transport of phytoplankton and nutrients. Flow discharge for Lake Chaohu was simulated based on the hydrological model in the coupled model. Sediment nutrient fluxes were estimated using the sediment flux module in EFDC.

(2) Acceptable model performance. The study aimed to simulate the cause-effect relationship between seasonal HABs and nutrient conditions in the lake. In term of above research purpose, the performance of the coupled model was acceptable because spatial pattern and seasonal trend of HABs and nutrient conditions were captured (Fig. 3). The multi-site and multi-variable calibration results (Section 3.1) revealed its ability in simulating hydrological, hydrodynamic and water quality conditions in Lake Chaohu. Its acceptable performance in simulating Q, WL and WT revealed a reasonable simulation of the hydrological and hydrodynamic conditions.

Although the model performance was acceptable in this study, several future works were recommended to improve model fit and

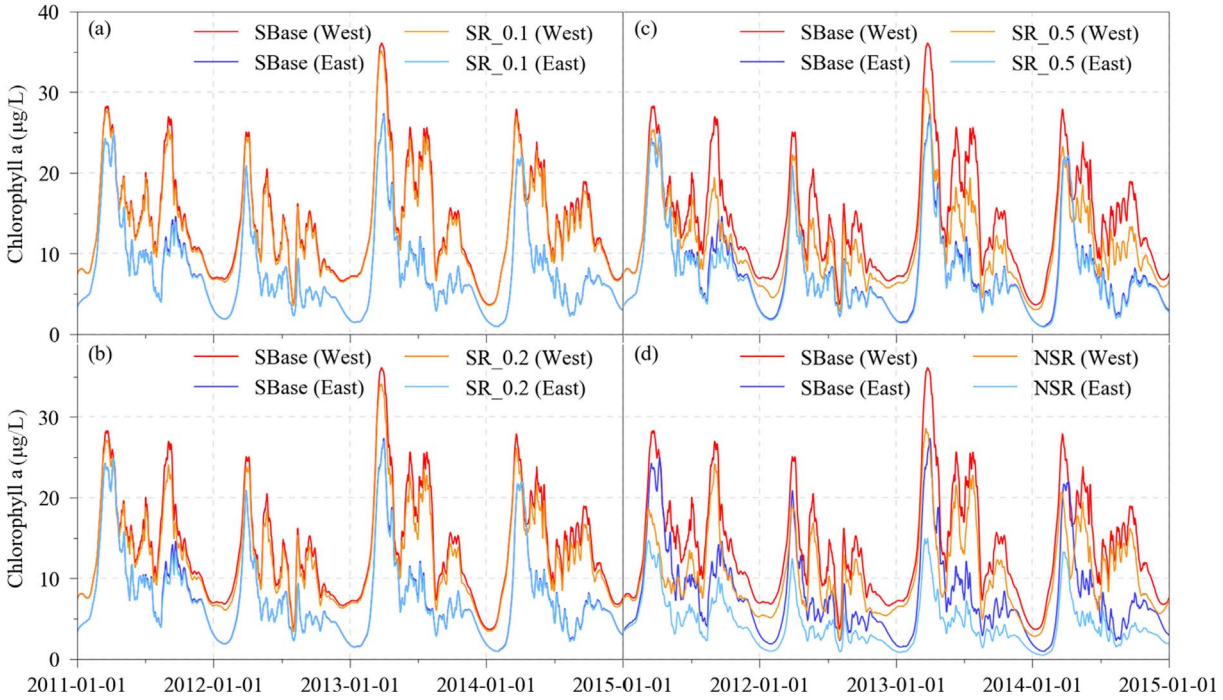

Fig. 5. Comparison of the spatially averaged chlorophyll *a* (μg/L) in the western and eastern Lake Chaohu for the period from Jan. 1, 2011 to Dec. 31, 2014 from five simulations: (a) SR_0.1 and SBase; (b) SR_0.2 and SBase; (c) SR_0.5 and SBase; (d) NSR and SBase. The geographic extents of the western and eastern Lake Chaohu can be found in Fig. 1. Simulation descriptions can be found in Table 2.

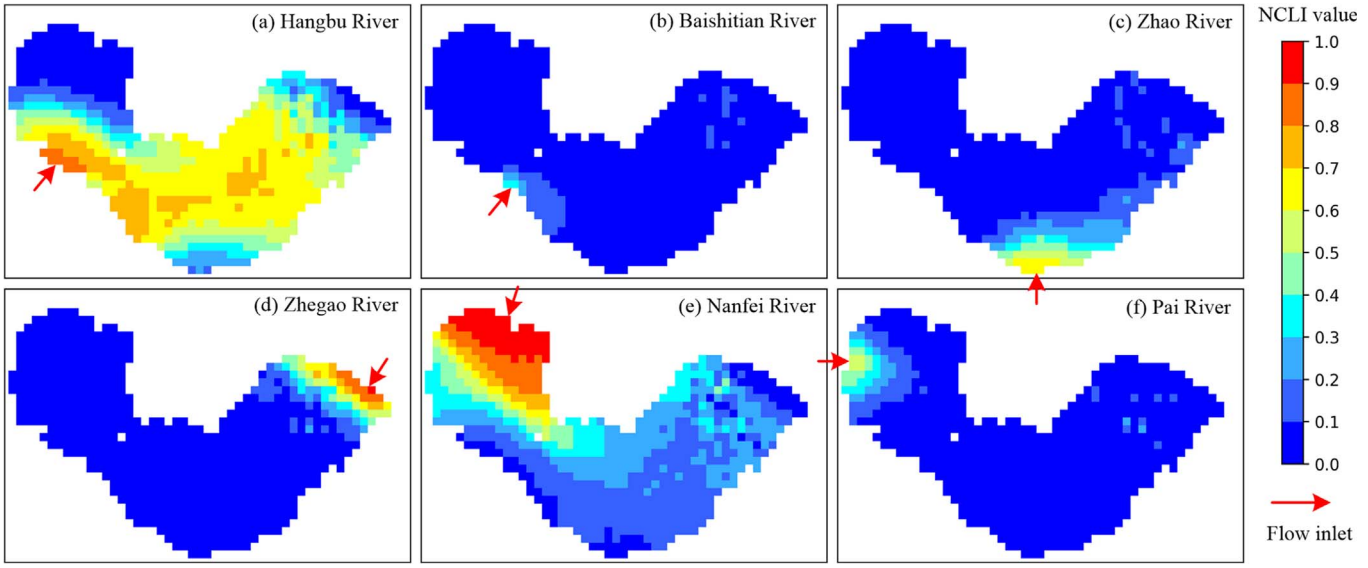

Fig. 6. The nutrient loading contribution index (NLCI) values of six inflows for Lake Chaohu: (a) Hangbu River; (b) Baishitian River; (c) Zhao River; (d) Zhegao River; (e) Nanfei River; (f) Pai River. See Fig. 1 for the geographical locations of these six inflows. Inlet for each inflow was marked with a red arrow. NLCI was calculated by Eq. (3) with the simulation chlorophyll *a* (μg/L) in the period from Jan. 1, 2011 to Dec. 31, 2014.

reduce model uncertainty.

(a) Reducing data uncertainty. The low model fit values for CHL, NH_4^+, TN and TP (Fig. 3) implied considerable uncertainty for the lake water quality model. We suggested paying more attention to data uncertainty in this case study. For example, daily wind conditions were used in this study. However, wind conditions may change significantly within a day. Moreover, inflow water quality data from monthly measurement (Table 1) were used as the boundary conditions for lake water quality model. However, water quality data from monthly sampling of inflows did not well reflect their temporal dynamics. To overcome this weakness, future work, such as coupling our developed model with a watershed model, is encouraged to estimate the time series data of watershed nutrient loading (Wellen et al., 2015).

(b) Improving underlying mechanism of the model. The vertical migration of phytoplankton was not adequately described in EFDC due to the lack of its underlying mechanism. However, it is clear that there is a vertical (upward and downward) migration for phytoplankton (e.g., cyanobacteria and diatoms), especially during the calm water flow periods in summer (Hu et al., 2016; Schaeffer et al., 2009). The vertical migration can lead to short-term algae accumulation on surface. Integrating the vertical migration mechanism of phytoplankton with EFDC is thus helpful for an accurate prediction of lake HABs.

(c) Further Validation on phytoplankton distribution and nutrient fluxes from sediments. The horizontal transport of phytoplankton was not adequately validated in this study due to the limited data to reflect the spatial distribution of phytoplankton. To overcome this data-limited weakness, future work on estimating phytoplankton distribution from satellite images was strongly encouraged (Hu et al., 2010). As shown in Fig. 5(d), nutrient fluxes have considerable impact on HABs, and were estimated based on the sediment flux module. However, an independent calibration and validation on this module was not implemented, and may result in considerable uncertainties in the estimated nutrient flux rate from sediments.

4.2. What is the prior nutrient to reduce: N or P?

Aquatic scientists were still debating the strategy of nutrient reduction for eutrophic lake among N control, P control and dual nutrient control strategies (Conley et al., 2009; Paerl et al., 2016; Schindler et al., 2016). To control HABs in Lake Chaohu, P should be reduced due to the following facts: (1) The high measured and simulation N:P ratio (> 10) in this study revealed that phytoplankton growth in Lake Chaohu was limited by P rather than N. (2) The monthly measured data during 2011–2014 showed a high N:P ratio (> 16) of six inflows for Lake Chaohu. (3) N-fixing phytoplankton community (*Anabaena*) was one of the dominant phytoplankton groups in Lake Chaohu (Zhang et al., 2016). This implied that considerable N can be obtained from atmospheric N_2. The finding of P limitation for HABs was consistent with previous studies based on measured data in Lake Chaohu (Zhang et al., 2016).

In this study, P controlling was proposed in Lake Chaohu. However, it is important to note that the prior nutrient to reduce can vary in different lakes. Therefore, it is widely encouraged to model lake eutrophication before take strategies (Bryhn and Håkanson, 2009).

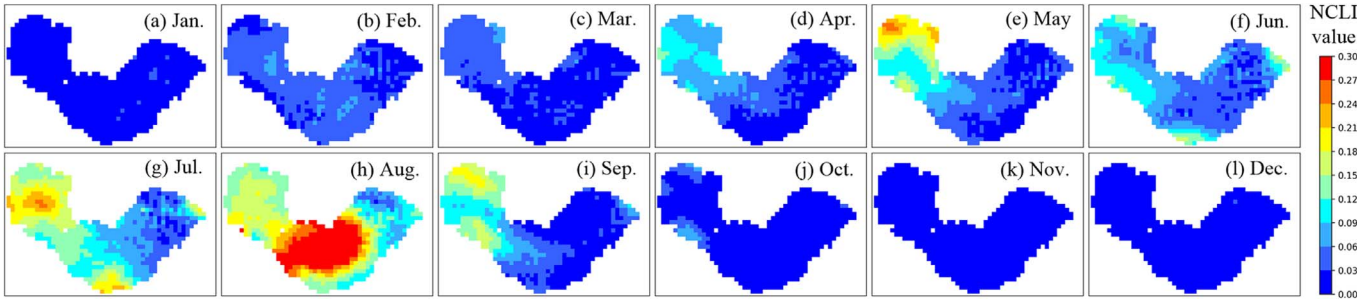

Fig. 7. The nutrient loading contribution index (NLCI) values of 12 months for Lake Chaohu: (a) Jan.; (b) Feb.; (c) Mar.; (d) Apr.; (e) May; (f) Jun.; (g) Jul.; (h) Aug.; (i) Sep.; (j) Oct.; (k) Nov.; (l) Dec. NLCI was calculated by Eq. (4) with the simulation chlorophyll a (μg/L) in the period from Jan. 1, 2011 to Dec. 31, 2014.

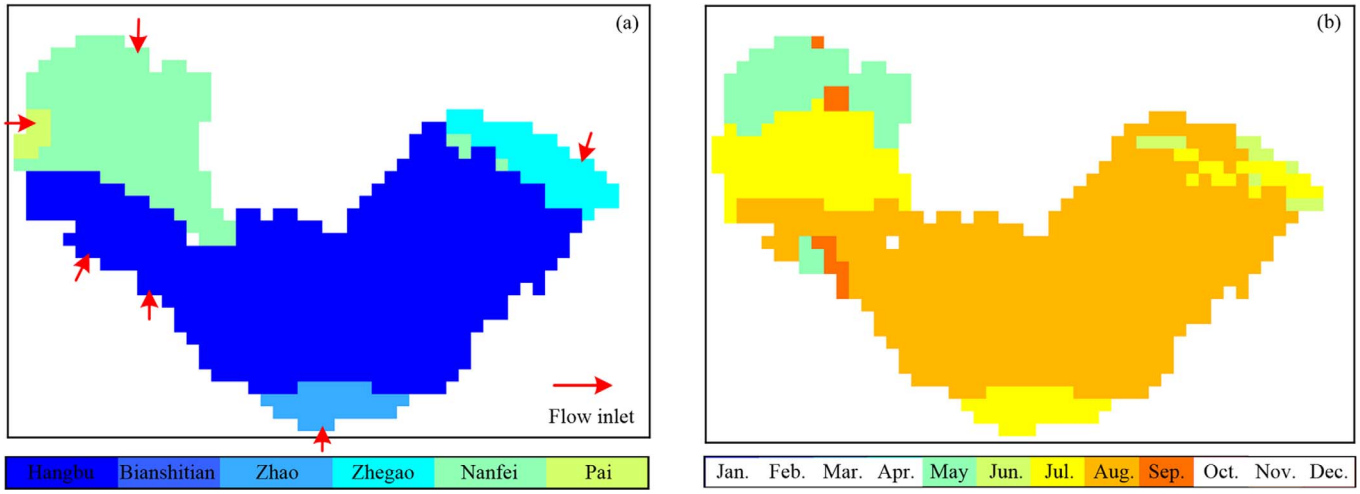

Fig. 8. Inflow and monthly contribution maps to represent the most important inflow and month for P reduction to control HABs in Lake Chaohu. The left figure (a) was generated by Eq. (5) with the nutrient loading contribution index (NLCI) values of six inflows for Lake Chaohu in Fig. 6. Inlet for each inflow was marked with a red arrow. The lake was divided into several zones. HABs in each zone were most sensitive to P reduction of an inflow (see the horizontal bar). The right figure (b) was generated by Eq. (6) with the nutrient loading contribution index (NLCI) values of 12 months for Lake Chaohu in Fig. 7. The lake was divided into several zones. HABs in each zone were most sensitive to P reduction of a month (see the horizontal bar).

4.3. What are the hot spots and hot moments of nutrient loading?

Six inflows' NLCI maps (Fig. 6) and the inflow contribution map (Fig. 8(a)) revealed the hot spots of nutrient loading for HABs in Lake Chaohu. The large spatial variations of NLCI maps implied that the hot spots of nutrient loading depended on the target lake areas to control HABs. To alleviate HABs in the western lake, reducing inflow TP loading from Nanfei River and internal TP loading was most important. To control HABs in the eastern lake, reducing inflow TP loading from Hangbu River and internal TP loading was most important. These identification results highlighted the necessity of considering spatial difference in learning the response of HABs to nutrient reduction in a large lake. Based on the identified hot spots of nutrient loading, the water managers can make a priority list for nutrient reduction in the lake.

The NLCI maps for 12 months (Fig. 7) and the monthly contribution map (Fig. 8(b)) revealed that the hot moments of TP loading for HABs in Lake Chaohu were Aug., May and Jul. Nutrients, temperature and light were considered to be the limitation factor for phytoplankton growth (Alex Elliott, 2012; Bleiker and Schanz, 1997). During the hot moments of TP loading (Aug., May and Jul.), water temperature and light intensity was close to their optimal conditions implying less limitation of phytoplankton growth by water temperature and light. TP was thus a critical factor affecting HABs.

This study compared the relative importance of nutrient reduction to control HABs among different flows and months. However, this does not mean that nutrient reduction is not necessary for the non-sensitive flows and during the non-sensitive periods. From the long-term view, all nutrient loadings into the lake can potentially increase HABs in case that they do not flow out of the lake.

4.4. What is the potential of nutrient loading contribution index

The proposed index (NLCI) had the advantage of representing the nutrient loading contribution to lake HABs in an explicit manner. This advantage mainly came from the potential of the hydrological, hydrodynamic and water quality model in simulating horizontal mass (nutrients and phytoplankton) transport within the lake, and cause-effect relationships between lake and watershed. NLCI was particularly useful for large eutrophic lakes with complex river network connected with them. The evaluation results using NLCI can support water managers in taking effective strategies to reduce nutrient loading for controlling lake HABs. For a proper use of NLCI in another lake, it is important to note that model calibration should be carried out based on measured data in the lake. Considering that the calculation of NLCI was relied on the hydrological, hydrodynamic and water quality model, continuing efforts was strongly encouraged to improve model fit and reduce model uncertainties.

5. Conclusions

A new index (NLCI) was proposed in this study to evaluate the contribution of nutrient loading on spatio-temporal pattern of HABs in Lake Chaohu. The index can be potentially used in other large eutrophic lakes, and support water management in several perspectives including: (1) improving our understanding on the response of HABs to nutrient reduction, (2) identifying the hot spots and moments to reduce nutrients for controlling HABs in a specific lake area, (3) and supporting water managers to make a prior list in reducing P loading.

Acknowledgments

We would like to thank editor and reviewers for their helpful comments. The project was financially supported by Major Science and Technology Program for Water Pollution Control and Treatment of China (2012ZX07501-001-03 and 2012ZX07506-001). The authors would like to thank China Meteorological Data Sharing Service System and Ministry of Environmental Protection of the People's Republic of China for providing the measured data for model development. Special thanks to China Scholarship Council for providing fellowship to visit the Ecological Modelling Laboratory in University of Toronto, Canada. Special thanks to Dr. Rui Zou (Tetra Tech, Inc., USA), Prof. Jian Shen (Virginia Institute of Marine Science, USA) and Dr. Scott C. James (Baylor University, USA) for their helps on lake modeling.

Appendix A. Supplementary data

Supplementary data associated with this article can be found, in the online version, at http://dx.doi.org/10.1016/j.ecolind.2018.01.056.

References

Abell, J.M., Özkundakci, D., Hamilton, D.P., 2010. Nitrogen and phosphorus limitation of phytoplankton growth in New Zealand Lakes: implications for eutrophication control.

Ecosystems 13, 966–977.
Alex Elliott, J., 2012. Predicting the impact of changing nutrient load and temperature on the phytoplankton of England's largest lake, Windermere. Freshwater Biol. 57, 400–413.
Allen, R.G., Pereira, L.S., Raes, D., Smith, M., 1998. Crop Evapotranspiration-Guidelines for Computing Crop Water Requirements. Food and Agriculture Organization of the United Nations D05109.
Andrews, D.M., Lin, H., Zhu, Q., Jin, L., Brantley, S.L., 2011. Hot spots and hot moments of dissolved organic carbon export and soil organic carbon storage in the shale hills catchment all rights reserved. No part of this periodical may be reproduced or transmitted in any form or by any means, electronic or mechanical, including photocopying, recording, or any information storage and retrieval system, without permission in writing from the publisher. Vadose Zone J. 10, 943–954.
Arifin, R.R., James, S.C., de Alwis Pitts, D.A., Hamlet, A.F., Sharma, A., Fernando, H.J.S., 2016. Simulating the thermal behavior in Lake Ontario using EFDC. J. Great Lakes Res. 42, 511–523.
Arrigo, K., 2014. Eighty years of Redfield. Nat. Geosci. 7, 849.
Bleiker, W., Schanz, F., 1997. Light climate as the key factor controlling the spring dynamics of phytoplankton in Lake Zürich. Aquat. Sci. 59, 135–157.
Brookes, J.D., Carey, C.C., 2011. Resilience to blooms. Science 334, 46–47.
Bryhn, A.C., Håkanson, L., 2009. Eutrophication: model before acting. Science 324, 723.
Catherine, Q., Susanna, W., Isidora, E.-S., Mark, H., Aurélie, V., Jean-François, H., 2013. A review of current knowledge on toxic benthic freshwater cyanobacteria – ecology, toxin production and risk management. Water Res. 47, 5464–5479.
Clark, J.M., Schaeffer, B.A., Darling, J.A., Urquhart, E.A., Johnston, J.M., Ignatius, A.R., Myer, M.H., Loftin, K.A., Werdell, P.J., Stumpf, R.P., 2017. Satellite monitoring of cyanobacterial harmful algal bloom frequency in recreational waters and drinking water sources. Ecol. Indic. 80, 84–95.
Conley, D.J., Paerl, H.W., Howarth, R.W., Boesch, D.F., Seitzinger, S.P., Havens, K.E., Lancelot, C., Likens, G.E., 2009. Controlling eutrophication: nitrogen and phosphorus. Science 323, 1014–1015.
Du, J., Shen, J., 2016. Water residence time in Chesapeake Bay for 1980–2012. J. Mar. Syst. 164, 101–111.
Hamrick, J.M., 1996. User's manual for the environmental fluid dynamics computer code. Department of Physical Sciences, School of Marine Science, Virginia Institute of Marine Science, College of William and Mary.
Hecky, R., Kilham, P., 1988. Nutrient limitation of phytoplankton in freshwater and marine environments: a review of recent evidence on the effects of enrichment. Limnol. Oceanogr. 33, 796–822.
Hu, C., Barnes, B.B., Qi, L., Lembke, C., English, D., 2016. Vertical migration of Karenia brevis in the northeastern Gulf of Mexico observed from glider measurements. Harmful Algae 58, 59–65.
Hu, C., Lee, Z., Ma, R., Yu, K., Li, D., Shang, S., 2010. Moderate resolution imaging spectroradiometer (MODIS) observations of cyanobacteria blooms in Taihu Lake, China. J. Geophys. Res. 115, C04002.
Huang, J., Gao, J., Hörmann, G., 2012. Hydrodynamic-phytoplankton model for short-term forecasts of phytoplankton in Lake Taihu, China. Limnologica 42, 7–18.
Huang, J., Gao, J., Zhang, Y., Xu, Y., 2015. Modeling impacts of water transfers on alleviation of phytoplankton aggregation in Lake Taihu. J. Hydroinform. 17, 149–162.
Huang, J., Qi, L., Gao, J., Kim, D.-K., 2017. Risk assessment of hazardous materials loading into four large lakes in China: a new hydrodynamic indicator based on EFDC. Ecol. Indic. 80, 23–30.
Huang, L., Fang, H., He, G., Jiang, H., Wang, C., 2016. Effects of internal loading on phosphorus distribution in the Taihu Lake driven by wind waves and lake currents. Environ. Pollut. 219, 760–773.
Imboden, D.M., Gachter, R., 1978. A dynamic lake model for trophic state prediction. Ecol. Model. 4, 77–98.
Jiang, Y., He, W., Liu, W., Qin, N., Ouyang, H., Wang, Q., Kong, X., He, Q., Yang, C., Yang, B., Xu, F., 2014. The seasonal and spatial variations of phytoplankton community and their correlation with environmental factors in a large eutrophic Chinese lake (Lake Chaohu). Ecol. Indic. 40, 58–67.
Kong, X., He, Q., Yang, B., He, W., Xu, F., Janssen, A.B.G., Kuiper, J.J., van Gerven, L.P.A., Qin, N., Jiang, Y., Liu, W., Yang, C., Bai, Z., Zhang, M., Kong, F., Janse, J.H., Mooij, W.M., 2017. Hydrological regulation drives regime shifts: evidence from paleolimnology and ecosystem modeling of a large shallow Chinese lake. Glob. Change Biol. 23, 737–754.
Krause, P., Boyle, D., Bäse, F., 2005. Comparison of different efficiency criteria for hydrological model assessment. Adv. Geosci. 5, 89–97.
Michalak, A.M., Anderson, E.J., Beletsky, D., Boland, S., Bosch, N.S., Bridgeman, T.B., Chaffin, J.D., Cho, K., Confesor, R., Daloğlu, I., DePinto, J.V., Evans, M.A., Fahnenstiel, G.L., He, L., Ho, J.C., Jenkins, L., Johengen, T.H., Kuo, K.C., LaPorte, E., Liu, X., McWilliams, M.R., Moore, M.R., Posselt, D.J., Richards, R.P., Scavia, D., Steiner, A.L., Verhamme, E., Wright, D.M., Zagorski, M.A., 2013. Record-setting algal bloom in Lake Erie caused by agricultural and meteorological trends consistent with expected future conditions. Proc. Natl. Acad. Sci. 110, 6448–6452.
National Research Council, 1992. Restoration of Aquatic Ecosystem. National Research Council National Academy Press, Washington, D.C.
Paerl, H.W., Huisman, J., 2008. Blooms like it hot. Science 320, 57–58.
Paerl, H.W., Scott, J.T., McCarthy, M.J., Newell, S.E., Gardner, W.S., Havens, K.E., Hoffman, D.K., Wilhelm, S.W., Wurtsbaugh, W.A., 2016. It takes two to tango: when and where dual nutrient (N & P) reductions are needed to protect lakes and downstream ecosystems. Environ. Sci. Technol. 50, 10805–10813.
Park, K., Jung, H.-S., Kim, H.-S., Ahn, S.-M., 2005. Three-dimensional hydrodynamic-eutrophication model (HEM-3D): application to Kwang-Yang Bay, Korea. Mar. Environ. Res. 60, 171–193.
Qin, B., Zhu, G., Gao, G., Zhang, Y., Li, W., Paerl, H.W., Carmichael, W.W., 2010. A drinking water crisis in Lake Taihu, China: linkage to climatic variability and lake management. Environ. Manage. 45, 105–112.
Schaeffer, B.A., Kamykowski, D., Sinclair, G., McKay, L., Milligan, E.J., 2009. Diel vertical migration thresholds of Karenia brevis (Dinophyceae). Harmful Algae 8, 692–698.
Schindler, D.W., 1974. Eutrophication and recovery in experimental lakes: implications for lake management. Science 184, 897–899.
Schindler, D.W., Carpenter, S.R., Chapra, S.C., Hecky, R.E., Orihel, D.M., 2016. Reducing phosphorus to Curb lake eutrophication is a success. Environ. Sci. Technol. 50, 8923–8929.
Schindler, D.W., Hecky, R.E., Findlay, D.L., Stainton, M.P., Parker, B.R., Paterson, M.J., Beaty, K.G., Lyung, M., Kasian, S.E.M., 2008. Eutrophication of lakes cannot be controlled by reducing nitrogen input: results of a 37-year whole-ecosystem experiment. Proc. Natl. Acad. Sci. 105, 11254–11258.
Schindler, D.W., Hecky, R.E., McCullough, G.K., 2012. The rapid eutrophication of Lake Winnipeg: greening under global change. J. Great Lakes Res. 38 (Suppl. 3), 6–13.
Shimoda, Y., Watson, S.B., Palmer, M.E., Koops, M.A., Mugalingam, S., Morley, A., Arhonditsis, G.B., 2016. Delineation of the role of nutrient variability and dreissenids (Mollusca, Bivalvia) on phytoplankton dynamics in the Bay of Quinte, Ontario, Canada. Harmful Algae 55, 121–136.
Smith, D.R., King, K.W., Williams, M.R., 2015. What is causing the harmful algal blooms in Lake Erie? J. Soil Water Conserv. 70, 27A–29A.
Tang, T.J., Yang, S., Peng, Y., Yin, K., Zou, R., 2017. Eutrophication control decision making using EFDC model for Shenzhen Reservoir, China. Water Resour. 44, 308–314.
Tetra Tech, I., 2007. The Environmental Fluid Dynamics Code: Theory and Computation. US EPA, Fairfax, VA.
Thomas, E.A., 1972. Phosphate removal by recirculating iron sludge. J. Water Pollut. Control Fed. 44, 176–182.
Ulrich, A.E., Malley, D.F., Watts, P.D., 2016. Lake Winnipeg Basin: advocacy, challenges and progress for sustainable phosphorus and eutrophication control. Sci. Total Environ. 542 (Part B), 1030–1039.
Vollenweider, R.A., 1976. Advances in defining critical loading levels for phosphorus in lake eutrophication. Mem. Ist. Ital. Idrobiol. 33, 53–83.
Watson, S.B., Miller, C., Arhonditsis, G., Boyer, G.L., Carmichael, W., Charlton, M.N., Confesor, R., Depew, D.C., Höök, T.O., Ludsin, S.A., Matisoff, G., McElmurry, S.P., Murray, M.W., Peter Richards, R., Rao, Y.R., Steffen, M.M., Wilhelm, S.W., 2016. The re-eutrophication of Lake Erie: harmful algal blooms and hypoxia. Harmful Algae 56, 44–66.
Wellen, C., Kamran-Disfani, A.-R., Arhonditsis, G.B., 2015. Evaluation of the current state of distributed watershed nutrient water quality modeling. Environ. Sci. Technol. 49, 3278–3290.
Wu, Z., Liu, Y., Liang, Z., Wu, S., Guo, H., 2017. Internal cycling, not external loading, decides the nutrient limitation in eutrophic lake: a dynamic model with temporal Bayesian hierarchical inference. Water Res. 116, 231–240.
Xu, F., Jørgensen, S.E., Tao, S., Li, B., 1999. Modeling the effects of ecological engineering on ecosystem health of a shallow eutrophic Chinese lake (Lake Chao). Ecol. Model. 117, 239–260.
Zhang, M., Zhang, Y., Yang, Z., Wei, L., Yang, W., Chen, C., Kong, F., 2016. Spatial and seasonal shifts in bloom-forming cyanobacteria in Lake Chaohu: patterns and driving factors. Phycol. Res. 64, 44–55.
Zhang, Y., Ma, R., Zhang, M., Duan, H., Loiselle, S., Xu, J., 2015. Fourteen-year record (2000–2013) of the spatial and temporal dynamics of floating algae blooms in Lake Chaohu, observed from time series of MODIS images. Remote Sens. 7, 10523.
Zhao, G., Hörmann, G., Fohrer, N., Gao, J., Li, H., Tian, P., 2011. Application of a simple raster-based hydrological model for streamflow prediction in a humid catchment with polder systems. Water Resour. Manage. 25, 661–676.
Zhao, R., 1992. The Xinanjiang model applied in China. J. Hydrol. 135, 371–381.
Zhou, H., Gao, C., 2011. Assessing the risk of phosphorus loss and identifying critical source areas in the Chaohu Lake Watershed, China. Environ. Manage. 48, 1033.
Zhu, M., Paerl, H.W., Zhu, G., Wu, T., Li, W., Shi, K., Zhao, L., Zhang, Y., Qin, B., Caruso, A.M., 2014. The role of tropical cyclones in stimulating cyanobacterial (Microcystis spp.) blooms in hypertrophic Lake Taihu, China. Harmful Algae 39, 310–321.